

Heat Transfer from each surface for a 3-D Thermally Asymmetric Rectangular Fin

Hyung Suk Kang

Abstract

The non-dimensional convective heat losses from each surface are investigated as a function of the non-dimensional fin length, width and the ratio of upper surface Biot number to bottom surface Biot number (Bi_2/Bi_1) using the three-dimensional separation of variables method. Heat loss ratio in view of each surface with the variation of Bi_2/Bi_1 is presented. The variation of the non-dimensional temperature profile along the fin center line for a thermally asymmetric conditions is also presented.

1. Introduction

Fins are widely used to enhance the rate of heat transfer to a surrounding fluid in many industrial applications such as electronic equipments, many kind of heat exchangers, air craft and so on. As a result, a great deal of attention has been directed to fin problems and various shapes of fins have been studied. For example, Sen and Trinh (1986), Look (1988) have discussed rectangular, Burmeister (1979) and Abrate and Newnham (1995) were concerned with triangular while Kang and Look (1999) and Kraus et al. (1978) examined trapezoidal. Finally Kim and Kang (1998) presented parabolic fin and Ullmann and Kalman (1989) researched annular fins. Usually most of the studies on the fin assume that the heat transfer coefficients for all surfaces of the fin are the same. But no literature seems to be available which presents a rectangular fin with unequal heat transfer coefficients by using a three dimensional analysis.

This paper presents an analysis of heat transfer from each surface for a three dimensional thermally asymmetric rectangular fin. In this study the upper surface Biot number, Bi_1 , is equal to or larger than the bottom surface Biot number, Bi_2 and the left surface Biot number, Bi_3 , is equal to or larger than the right surface Biot number, Bi_4 , and Bi_5 , at the fin tip, has various values. The non-dimensional heat losses from each surface are investigated as a function of the non-dimensional fin length, width and the Bi_2/Bi_1 ratio using the three-dimensional separation of variables method. Heat loss ratio in view of each surface with the variation of Bi_2/Bi_1 is presented. The variation of the non-dimensional

Key words: 3-D analytical method, Heat transfer coefficient, Heat loss, Biot number

temperature profile along the fin center line for a thermally asymmetric conditions is also presented. For simplicity, the root temperature and the thermal conductivity of the fin's material are assumed constant as well as steady-state.

Nomenclature

- Bi_1 : fin upper surface Biot number, $h_1 l / k$
 Bi_2 : fin bottom surface Biot number, $h_2 l / k$
 Bi_3 : fin left surface Biot number, $h_3 l / k$
 Bi_4 : fin right surface Biot number, $h_4 l / k$
 Bi_5 : fin tip surface Biot number, $h_5 l / k$
 h_1 : fin upper surface heat transfer coefficient [$W/m^2 \text{ } ^\circ C$]
 h_2 : fin bottom surface heat transfer coefficient [$W/m^2 \text{ } ^\circ C$]
 h_3 : fin left surface heat transfer coefficient [$W/m^2 \text{ } ^\circ C$]
 h_4 : fin right surface heat transfer coefficient [$W/m^2 \text{ } ^\circ C$]
 h_5 : fin tip surface heat transfer coefficient [$W/m^2 \text{ } ^\circ C$]
 k : thermal conductivity [$W/m \text{ } ^\circ C$]
 l : one half fin height at the base [m]
 L' : fin length (base to tip) [m]
 L : non-dimensional fin length, L' / l
 Q : heat loss from a rectangular fin [W]
 Q_{us} : convective heat loss from upper surface [W]
 Q_{bs} : convective heat loss from bottom surface [W]
 Q_{ls} : convective heat loss from left surface [W]
 Q_{rs} : convective heat loss from right surface [W]
 Q_{ts} : convective heat loss from tip surface [W]
 T : fin temperature [$^\circ C$]
 T_w : fin base temperature [$^\circ C$]
 T_∞ : ambient temperature [$^\circ C$]
 w' : one half fin width [m]
 w : non-dimensional a half fin width, w' / l
 x' : length directional variable [m]
 x : non-dimensional length directional variable, x' / l
 y' : height directional variable [m]
 y : non-dimensional height directional variable, y' / l
 z' : width directional variable [m]
 z : non-dimensional width directional variable, z' / l
 θ_0 : adjusted temperature, $(T_w - T_\infty)$
 θ : non-dimensional temperature, $(T - T_\infty) / (T_w - T_\infty)$
 λ_m : eigenvalues ($m = 1, 2, 3, \dots$)

μ_n : eigenvalues ($n = 1, 2, 3, \dots$)

ρ_{nm} : eigenvalues ($= \sqrt{\lambda_m^2 + \mu_n^2}$)

2. Three-Dimensional Analysis

Geometry of a rectangular fin with all different heat transfer coefficients is shown in Fig. 1. Three-dimensional governing differential equation under steady state for this figure is

$$\frac{\partial^2 \theta}{\partial x^2} + \frac{\partial^2 \theta}{\partial y^2} + \frac{\partial^2 \theta}{\partial z^2} = 0. \tag{1}$$

Six boundary conditions are required to solve the equation (1). These conditions are shown as equations (2)~(7).

$$\theta = 1 \quad \text{at } x = 0 \tag{2}$$

$$\frac{\partial \theta}{\partial x} + Bi5 \cdot \theta = 0 \quad \text{at } x = L \tag{3}$$

$$\frac{\partial \theta}{\partial y} + Bi1 \cdot \theta = 0 \quad \text{at } y = 1 \tag{4}$$

$$\frac{\partial \theta}{\partial y} - Bi2 \cdot \theta = 0 \quad \text{at } y = -1 \tag{5}$$

$$\frac{\partial \theta}{\partial z} + Bi3 \cdot \theta = 0 \quad \text{at } z = w \tag{6}$$

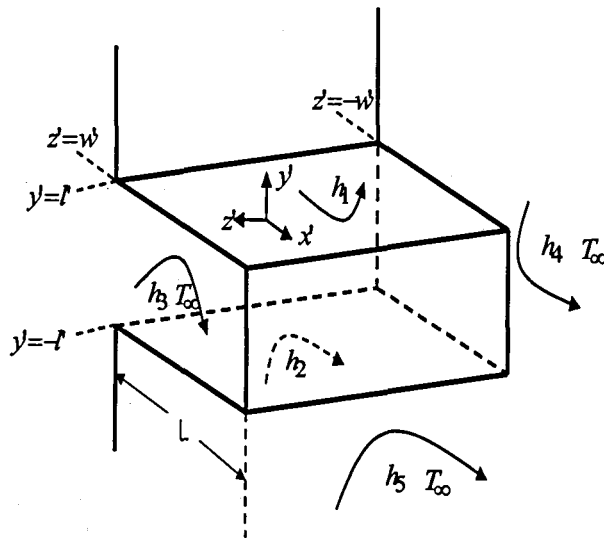


Fig. 1 Geometry of a thermally asymmetric rectangular fin

$$\frac{\partial \theta}{\partial z} - Bi4 \cdot \theta = 0 \quad \text{at } z = -w \quad (7)$$

The solution for the non-dimensional temperature distribution $\theta(x, y, z)$ within the fin obtained with equations (2)~(5) is

$$\theta(x, y, z) = \sum_{n=1}^{\infty} \sum_{m=1}^{\infty} N_{nm} \cdot f(x) \cdot f(y) \cdot f(z) \quad (8)$$

where

$$N_{nm} = \frac{4 \sin(\lambda_n) \cdot \sin(\mu_m \cdot w)}{f_n \cdot g_m} \quad (9)$$

$$f(x) = \cosh(\rho_{nm} \cdot x) - C_{nm} \cdot \sinh(\rho_{nm} \cdot x) \quad (10)$$

$$C_{nm} = \frac{\rho_{nm} \cdot \tanh(\rho_{nm} \cdot L) + Bi5}{\rho_{nm} + Bi5 \cdot \tanh(\rho_{nm} \cdot L)} \quad (11)$$

$$\rho_{nm} = \sqrt{(\lambda_n^2 + \mu_m^2)} \quad (12)$$

$$f(y) = \cos(\lambda_n \cdot y) + A_n \cdot \sin(\lambda_n \cdot y) \quad (13)$$

$$A_n = \frac{\lambda_n \cdot \tan \lambda_n - Bi1}{\lambda_n + Bi1 \cdot \tan \lambda_n} \quad (14)$$

$$f(z) = \cos(\mu_m \cdot z) + B_m \cdot \sin(\mu_m \cdot z) \quad (15)$$

$$B_m = \frac{\mu_m \cdot \tan(\mu_m \cdot w) - Bi3}{\mu_m + Bi3 \cdot \sin(\mu_m \cdot w)} \quad (16)$$

$$f_n = \lambda_n + \frac{1}{2} \sin(2\lambda_n) + A_n^2 \cdot \left\{ \lambda_n - \frac{1}{2} \sin(2\lambda_n) \right\} \quad (17)$$

$$g_m = \mu_m w + \frac{1}{2} \sin(\mu_m w) + B_m^2 \cdot \left\{ \mu_m w - \frac{1}{2} \sin(\mu_m w) \right\} \quad (18)$$

The eigenvalues λ_n can be obtained from equation (19) which comes from equation (4) and equation (5).

$$\frac{\lambda_n \cdot \sin(\lambda_n) - Bi1 \cdot \cos(\lambda_n)}{\lambda_n \cdot \cos(\lambda_n) + Bi1 \cdot \sin(\lambda_n)} = \frac{Bi2 \cdot \cos(\lambda_n) - \lambda_n \cdot \sin(\lambda_n)}{\lambda_n \cdot \cos(\lambda_n) + Bi2 \cdot \sin(\lambda_n)} \quad (19)$$

The eigenvalues μ_m can be obtained from equation (20) which comes from equation (6) and equation (7).

$$\frac{\mu_m \cdot \sin(\mu_m \cdot w) - Bi3 \cdot \cos(\mu_m \cdot w)}{\mu_m \cdot \cos(\mu_m \cdot w) + Bi3 \cdot \sin(\mu_m \cdot w)} = \frac{Bi4 \cdot \cos(\mu_m \cdot w) - \mu_m \cdot \sin(\mu_m \cdot w)}{\mu_m \cdot \cos(\mu_m \cdot w) + Bi4 \cdot \sin(\mu_m \cdot w)} \quad (20)$$

By applying equation (8) to Fourier's law, the heat loss rate conducted into the fin through the fin base is given by equation (21).

$$Q = 4k \cdot l \cdot \theta_0 \sum_{n=1}^{\infty} \sum_{m=1}^{\infty} N_{nm} \cdot \rho_{nm} \cdot C_{nm} \cdot \frac{\sin(\lambda_n)}{\lambda_n} \cdot \frac{\sin(\mu_m \cdot w)}{\mu_m} \quad (21)$$

Convective heat losses from each surface for a thermally asymmetric rectangular fin can be expressed equation (21) through equation (25).

$$\frac{Q_{us}}{kl\theta_0} = \sum_{n=1}^{\infty} \sum_{m=1}^{\infty} Bi1 \cdot N_{nm} \cdot D_{nm} \cdot (\cos \lambda_n + A_n \cdot \sin \lambda_n) \cdot \frac{2 \sin(\mu_m \cdot w)}{\mu_m} \quad (21)$$

$$\frac{Q_{bs}}{kl\theta_0} = \sum_{n=1}^{\infty} \sum_{m=1}^{\infty} Bi2 \cdot N_{nm} \cdot D_{nm} \cdot (\cos \lambda_n - A_n \cdot \sin \lambda_n) \cdot \frac{2 \sin(\mu_m \cdot w)}{\mu_m} \quad (22)$$

$$\frac{Q_{ls}}{kl\theta_0} = \sum_{n=1}^{\infty} \sum_{m=1}^{\infty} Bi3 \cdot N_{nm} \cdot D_{nm} \cdot (\cos \mu_m + B_m \cdot \sin \mu_m) \cdot \frac{2 \sin(\lambda_n)}{\lambda_n} \quad (23)$$

$$\frac{Q_{rs}}{kl\theta_0} = \sum_{n=1}^{\infty} \sum_{m=1}^{\infty} Bi4 \cdot N_{nm} \cdot D_{nm} \cdot (\cos \mu_m - B_m \cdot \sin \mu_m) \cdot \frac{2 \sin(\lambda_n)}{\lambda_n} \quad (24)$$

$$\frac{Q_{fs}}{kl\theta_0} = \sum_{n=1}^{\infty} \sum_{m=1}^{\infty} Bi5 \cdot N_{nm} \cdot E_{nm} \cdot \frac{\sin(\lambda_n)}{\lambda_n} \cdot \frac{\sin(\mu_m \cdot w)}{\mu_m} \quad (25)$$

where

$$D_{nm} = \frac{1}{\rho_{nm}} \cdot \frac{Bi5 \{ \cosh(\rho_{nm}L) - 1 \} + \rho_{nm} \cdot \sinh(\rho_{nm}L)}{\rho_{nm} \cdot \cosh(\rho_{nm}L) + Bi5 \cdot \sinh(\rho_{nm}L)} \quad (26)$$

$$E_{nm} = \frac{\rho_{nm}}{\rho_{nm} \cdot \cosh(\rho_{nm}L) + Bi5 \cdot \sinh(\rho_{nm}L)} \quad (27)$$

3. Results and Discussions

Figure 2 presents the convective heat losses from each surface of a thermally asymmetric rectangular fin as a function of the non-dimensional fin length for $Bi2/Bi1=0.8$, $Bi4/Bi3=0.9$, $Bi1=Bi3=Bi5=0.1$ and $w=0.5$. It is shown that the heat loss from the tip decreases while heat losses from all the other surfaces increase as the non-dimensional fin length increases. It can be noted that heat losses from upper and bottom surfaces are less than those from left and right surfaces because the fin width is comparatively narrow relative to the fin height.

Figures 3(a) shows the non-dimensional heat losses a unit width from each surface versus the non-dimensional fin length for $Bi1=Bi3=Bi5=0.01$, $Bi2/Bi1=Bi4/Bi3=0.9$ and $w=0.1$. The heat loss magnitude order and variation trend is somewhat similar to Fig. 2. The same condition except $w=2$ is described in Fig. 3(b). Comparing this figure to Fig. 3(a), heat loss from each surface varies more rapidly at a rate as the non-dimensional fin length increases and the order of heat loss magnitude between upper, bottom surfaces and left, right surfaces is

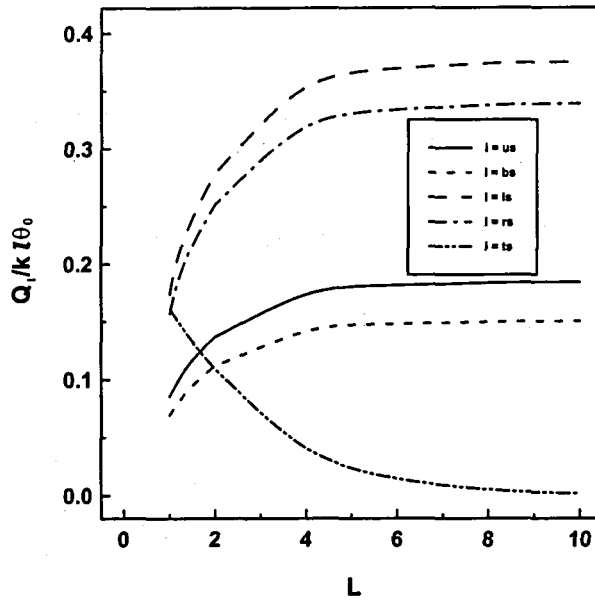


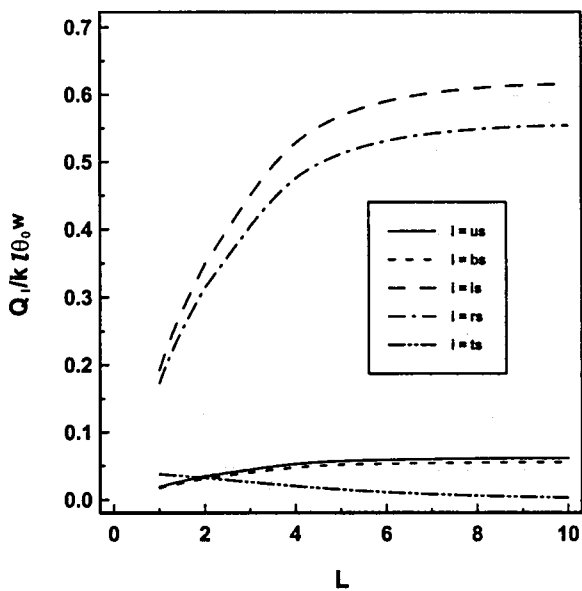
Fig. 2 Non-dimensional heat loss from each surface vs. L for $Bi_2/Bi_1=0.8$, $Bi_4/Bi_3=0.9$, $Bi_1=Bi_3=Bi_5=0.1$ and $w=0.5$

reversed because of width change. Also it can be noted that heat loss from the fin tip is the largest until the non-dimensional fin length increases to about 2.

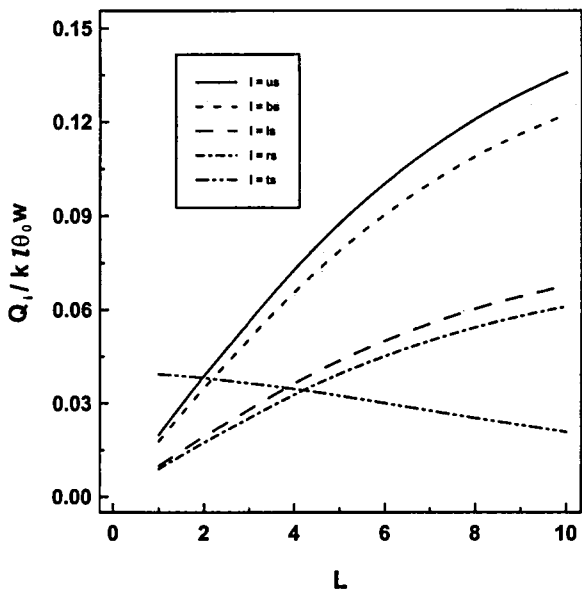
Figure 4 presents the non-dimensional heat losses from each surface versus the non-dimensional fin width for $Bi_1=Bi_3=Bi_5=0.01$, $Bi_2/Bi_1=Bi_4/Bi_3=0.9$ and $L=5$. Heat losses from left and right surfaces increase as w increases from 0.1 to 1 and then decrease as w increases from 1 to 10 while heat losses from upper, bottom and tip surfaces increase linearly as w increases from 0.1 to 10. It can be explained physically that the effect of heat loss from left and right surfaces on the total heat loss decreases as the fin width increases when the fin length is fixed.

Figure 5 illustrates the variation of the non-dimensional temperature along the fin center line for three different asymmetric condition in case of $Bi_1=Bi_3=Bi_5=0.02$, $L=5$ and $w=0.5$. Average surrounding Biot numbers are equal for three different conditions. The temperature difference increases as x coordinate increases. The temperature is the lowest in case of $Bi_2/Bi_1=0.2$, $Bi_4/Bi_3=1.0$ and it means physically that heat loss is the highest.

Table 1 lists the heat loss ratio in view of each surface with the



(a) $w=0.1$



(b) $w=2$

Fig. 3 Non-dimensional heat loss a unit width from each surface vs. L for $Bi_1=Bi_3=Bi_5=0.01$, $Bi_2/Bi_1=0.9$ and $Bi_4/Bi_3=0.9$

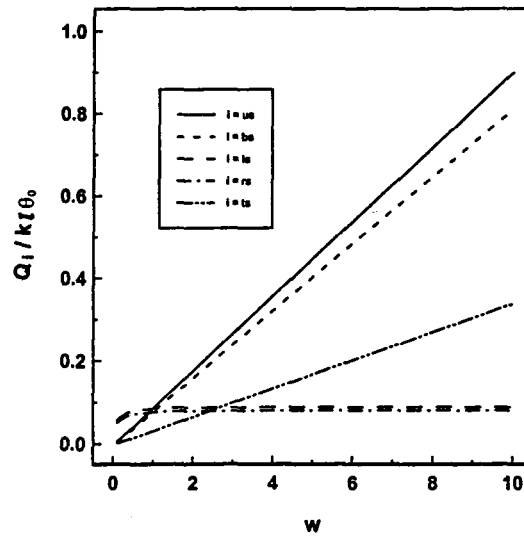


Fig. 4 Non-dimensional heat loss from each surface vs. w for $L=5$, $Bi_1=Bi_3=Bi_5=0.01$, and $Bi_2/Bi_1=Bi_4/Bi_3=0.9$

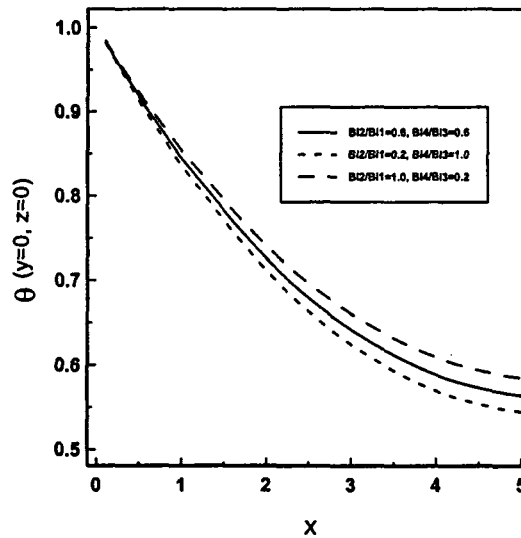


Fig. 5 Non-dimensional temperature along x coordinate for $L=5$, $w=0.5$ and $Bi_1=Bi_3=Bi_5=0.02$

Table 1 Heat loss ratio in view of each surface with the variation of Bi_2/Bi_1 for $Bi_1=Bi_3=Bi_5=0.05$, $Bi_4/Bi_3=0.8$, $L=5$ and $w=0.5$.

Bi_2/Bi_1	Q_{rs}/Q_{ls} (%)	Q_{bs}/Q_{us} (%)	Q_{us}/Q_{ls} (%)	Q_{ts}/Q_{ls} (%)
0.6	80.35	61.18	49.38	11.27
0.7	80.35	71.03	49.46	11.17
0.8	80.35	80.78	49.55	11.08
0.9	80.35	90.44	49.63	10.99
1.0	80.35	100.00	49.72	10.91

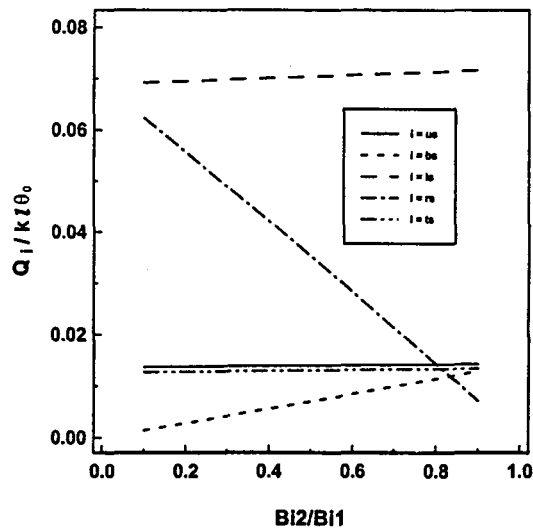


Fig. 6 Non-dimensional heat loss from each surface vs. Bi_2/Bi_1 for $Bi_1=Bi_3=Bi_5=0.02$, $w=0.2$, $L=2$ and $Bi_4/Bi_3=1-Bi_2/Bi_1$

variation of Bi_2/Bi_1 for $Bi_1=Bi_3=Bi_5=0.05$, $Bi_4/Bi_3=0.8$, $L=5$ and $w=0.5$. First it can be noted that the ratio of heat loss from right surface to that from left surface remains 80.35 %, which is slightly over 80 %, with the variation of Bi_2/Bi_1 since Bi_4/Bi_3 remains 0.8. The ratio of heat loss from bottom surface to that from upper surface varies in proportion to the ratio of Bi_2/Bi_1 but heat loss ratio is slightly higher

than the Biot number ratio and the difference between these two ratio decrease as Biot number ratio increases and it finally becomes 0 at $Bi_2/Bi_1=1$. It also describes heat loss from upper surface slightly less than half of that from left surface even though both surfaces have the same Biot number.

The non-dimensional heat losses from each surface versus Bi_2/Bi_1 for $Bi_1=Bi_3=Bi_5=0.02$, $Bi_4/Bi_3=1-Bi_2/Bi_1$, $w=0.2$ and $L=2$ are illustrated in Fig. 6. As expected, heat loss from bottom surface increases while that from right surface decreases as Bi_2/Bi_1 increases since Bi_4 decreases as Bi_2/Bi_1 increases. But it is interesting to note that heat losses from upper, left and tip surfaces increase as Bi_2/Bi_1 increases even though Bi_1 , Bi_3 and Bi_5 are constants.

4. Conclusions

The following conclusions can be made from the results.

- (1) Convective heat loss from fin tip increases as fin width increases while it decreases as fin length increases.
- (2) The ratio of heat loss from bottom surface to that from upper surface slightly higher than the ratio of Biot number of bottom surface to that of upper surface when this ratio (Bi_2/Bi_1) is not 1.
- (3) Heat losses from each surface vary linearly with the variations of Bi_2/Bi_1 and Bi_4/Bi_3 .

Reference

1. Abrate, S. and Newnham, P., "Finite Element Analysis of Triangular Fin Attached to a Thick Wall", *Computer & Structures*, Vol. 57, No. 6, 1995, pp. 945~957.
2. Burmeister, L. C., "Triangular Fin Performance by the Heat Balance Integral Method", *ASME J. Heat Trans.*, Vol. 101, 1979, pp. 562~564.
3. Kang, H. S. and Look, D. C., "A Comparison of Four Solution Methods for the Analysis of a Trapezoidal Fin", *KSME Int. Journal*, Vol. 13, No. 6, 1999, pp. 487~495.
4. Kim, K. T. and Kang, H. S., "A Heat Loss Comparison Between the Two Parabolic Fin Models using Two Different Numerical Methods", *J. of the KSIAM*, Vol. 2, No. 2, 1998, pp. 97~109.
5. Kraus, A. D., Snider, A. D. and Doty, L. F., "An Efficient Algorithm for Evaluating Arrays of Extended Surface", *ASME J. of Heat Trans.*, Vol. 100, 1978, pp. 288~293.
7. Look, D. C., "2-D Fin Performance: $Bi(\text{top}) > Bi(\text{bottom})$ ", *ASME J. of Heat Trans.*, Vol. 111, 1988, pp. 780~782.

8. Sen, A. K. and Trinh, S., "An Exact solution for the Rate of Heat Transfer from a Rectangular Fin Governed by a Power Law-Type Temperature Dependence", ASME J. of Heat Trans., Vol. 108, 1986, pp. 457~459.
9. Ullmann, A. and Kalman, H., "Efficiency and Optimized Dimensions of Annular Fins of Different Cross-Section Shapes", Int. J. Heat Mass Transfer, Vol. 32, 1989, pp. 1105~1110.

Division of Mechanical and Mechatronics Engineering
College of Engineering
Kangwon National University
Chunchon, Korea
hkang@cc.kangwon.ac.kr